

Integral Treatment for Heat and Mass Transfer by Natural Convection from a Horizontal Surface in a Radiating Darcian Fluid

Nasreen Bano¹ and B. B. Singh²

¹⁻²Department of Mathematics, Dr. Babasaheb Ambedkar Technological University, Lonere-402103
¹Email: snasreenbano@yahoo.in, ²Email: bbsingh@dbatu.ac.in

Abstract—This paper deals with the study of the heat and mass transfer characteristics of natural convection from a horizontal surface embedded in a radiating fluid saturated porous medium. Similarity solutions for buoyancy induced heat and mass transfer from a horizontal surface, where the wall temperature and concentration are a power function of distance from the origin, are obtained by using an integral approach of Von Karman type. The effects of the governing parameters such as buoyancy ratio, Lewis number, radiation parameter and the power-law exponent on local Nusselt and local Sherwood numbers have been investigated both numerically and graphically.

Index Terms— Buoyancy, Integral method, Heat transfer, Natural convection, Boundary layer thickness.

I. INTRODUCTION

Coupled heat and mass transfer (or double-diffusion) driven by buoyancy, due to temperature and concentration variations in a saturated porous medium, has several important applications in geothermal and geophysical engineering e.g. the migration of moisture in fibrous insulation and the underground disposal of nuclear wastes.

On account of the applications of the above mentioned phenomena in engineering and industrial processes, Cheng and Chang [1] investigated the buoyancy induced flows in a saturated porous medium adjacent to impermeable horizontal surfaces. Chang and Cheng [2] studied the matched asymptotic expansion for free convection about an impermeable horizontal surface in a porous medium. Bejan and Khair [3] investigated the vertical natural convection boundary layer flow in a saturated porous medium due to the combined heat and mass transfer. Jang and Chang [4] analyzed the buoyancy-induced inclined boundary layer flow in a saturated porous medium resulting from combined heat and mass buoyancy effects. Yücel [5-6] investigated the natural convection heat and mass transfer along a vertical cylinder in a porous medium. Trevisan and Bejan [7] analyzed the combined heat and mass transfer by natural convection in a porous medium. Nakayama and Hossain [8] and Singh and Queeny [9] used an integral method to revisit the problem of Bejan and Khair [3]. Lai et al. [10] investigated the problem of coupled heat and mass transfer by natural convection from slender body of revolution in a porous medium. Lai and Kulacki [11] made an in-depth

study of the coupled heat and mass transfer by natural convection from a sphere buried in an infinite porous medium. Lai [12] analyzed the coupled heat and mass transfer by natural convection from a horizontal line source in a saturated porous medium. Nakayama and Ashizawa [13] performed a boundary layer analysis of the combined heat and mass transfer by natural convection from a concentrated source in a saturated porous medium. Yih [14] studied the heat and mass transfer characteristics in natural convection flow over a truncated cone subjected to variable wall temperature / concentration or variable heat / mass flux embedded in porous media under the coupled heat and mass diffusion. Chamkha and Khaled [15] studied the non-similar hydromagnetic simultaneous heat and mass transfer by mixed convection from a vertical plate embedded in a uniform porous medium. Bansod et al. [16] studied the heat and mass transfer by natural convection from a horizontal surface embedded in a Darcian fluid saturated porous medium. Chamkha and Khaled [17] investigated the hydromagnetic simultaneous heat and mass transfer by mixed convection from a vertical plate embedded in a stratified porous medium with thermal dispersion effect. Singh et al. [18] studied the influence of lateral mass flux on a porous medium. Bansod [19] investigated the Darcy model for boundary layer flows in a horizontal porous medium induced by combined buoyancy forces. Bansod [20] studied the effects of blowing and suction on double-diffusion by mixed convection over inclined permeable surfaces. Postelnicu [21] studied the influence of chemical reaction on heat and mass transfer by natural convection from vertical surfaces in porous media considering Soret and Dufour effects. Shateyi [22] studied the thermal radiation and buoyancy effects on heat and mass transfer over a semi-infinite stretching surface with suction and blowing. Bansod and Jadhav [23] gave an integral treatment of combined heat and mass transfer by natural convection along a horizontal surface in porous medium. Singh and Chandarki [24] gave an integral treatment for the problem of coupled heat and mass transfer by natural convection from vertical cylinder embedded in a saturated porous medium. Beg et al. [25] studied chemically-reacting mixing convective heat and mass transfer along inclined and vertical plates with Soret and Dufour effects. Bansod and Jadhav [26] studied the effects of double stratification on mixed convection heat and mass transfer from a vertical surface in a fluid saturated porous medium. Tak et al. [27] studied the MHD free convection radiation interaction along a vertical surface embedded in a Darcian porous medium in presence of Soret and Dufour effects. Bansod and Ambedkar [28] gave an integral treatment for combined heat and mass transfer by mixed convection along vertical surface in a saturated porous medium.

In the context of space technology and in the processes involving high temperatures, the effects of radiation are of vital importance. Recent developments in hypersonic flights in the paper by Di Clemente [29], missile re-entry, rocket combustion chambers, power plants for inter-planetary flight and gas cooled nuclear reactors, have focused attention on thermal radiation as a mode of energy transfer, and emphasized the need for improved understanding of radiative transfer in these processes. The interaction of radiation with laminar free-convection heat transfer from a vertical plate was investigated by Cess [30] for an absorbing and emitting fluid in the optically thick regions, and used the approximate integral technique and first order profiles to solve the energy equation. Raptis [31] analyzed the thermal radiation and free convection flow through a porous medium bounded by a vertical infinite porous plate by using a regular perturbation technique. Hossain and Takhar [32] studied the radiation effects on mixed convection along a vertical plate with uniform surface temperature using the Keller Box finite difference method. In all these papers, the flow is considered to be steady. The unsteady flow past a moving plate in the presence of free convection and radiation were presented by Mansour [33]. Radiation and mass transfer effects on two dimensional flow past an impulsively started isothermal vertical plate were analyzed by Prasad et al. [34]. Babu et al. [35] performed a numerical analysis to study the effects of radiation and heat source / sink on the steady two-dimensional magnetohydrodynamic (MHD) boundary layer flow of heat and mass transfer past a shrinking sheet with wall mass suction.

The objective of the present paper is to provide an integral treatment of Von Karman type to heat and mass transfer by natural convection from horizontal surface in a radiating Darcian fluid. The effects of parameters like buoyancy ratio, Lewis number, radiation parameter and power law exponent on local Nusselt and local Sherwood numbers have been studied both numerically and graphically. Our results have been compared graphically with the already published results of Bansod et al. [16] who visited the same problem in the absence of radiative fluid properties by using shooting method aided by Runge-Kutta method. Our results have been found in excellent agreement. It has been concluded through our analysis that the radiation parameter has significant effects on the local Nusselt and local Sherwood numbers. In the analysis, the boundary layer equations are reduced to ordinary differential equations using similarity transformations. These transformations are valid for the power law exponent lying in the range $0 \leq n \leq 2$. It is further found

that the rates of heat and mass transfer increase as n increases. Furthermore, it has been found that these physical quantities show an increasing trend with buoyancy ratio (B) for the case of fixed Lewis number (Le), radiation parameter (R_d^*) and power law exponent (n).

II. PROBLEM FORMULATION

Let us consider the steady boundary layer flow of an incompressible fluid near an impermeable horizontal surface embedded in a saturated porous medium (Fig.1). The wall temperature and concentration have been assumed to be a power function of x i.e. $T_w = T_\infty + a x^n$ and $C_w = C_\infty + b x^n$, where a, b and n are the constants.

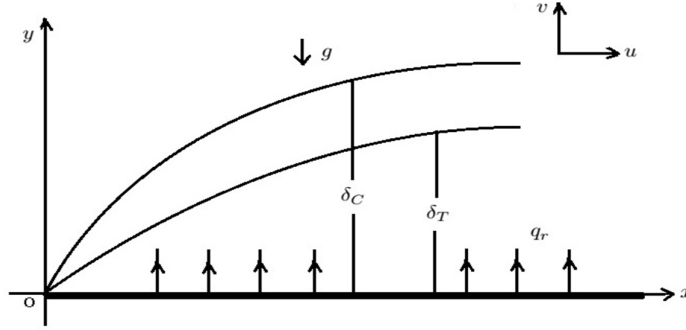


Figure 1. Temperature and concentration boundary layer along a horizontal surface

Here x represents the distance along the surface from its leading edge, and y the distance normal to the surface. In the analysis, all the physical properties of the fluid except the density- term associated with the body force have been assumed to be constant.

Further, the Darcy's law, the Boussinesq and boundary layer approximations have been assumed to hold true in the present analysis.

With these assumptions, the system of equations, which models the flow, are given by

$$\frac{\partial u}{\partial x} + \frac{\partial v}{\partial y} = 0, \quad (1)$$

$$\frac{\partial u}{\partial y} = -\frac{Kg}{\nu} \left[\beta_T \frac{\partial T}{\partial x} + \beta_C \frac{\partial C}{\partial x} \right], \quad (2)$$

$$u \frac{\partial T}{\partial x} + v \frac{\partial T}{\partial y} = \alpha \frac{\partial^2 T}{\partial y^2} - \frac{1}{\rho c_p} \frac{\partial q_r}{\partial y}, \quad (3)$$

$$u \frac{\partial C}{\partial x} + v \frac{\partial C}{\partial y} = D \frac{\partial^2 C}{\partial y^2}, \quad (4)$$

where u, v are the Darcian velocities in $x-, y-$ directions. Here β_T and β_C are the thermal and concentration coefficients, respectively and ν is the kinematic viscosity of the fluid. Furthermore, g is the gravitational acceleration, K is the permeability of the porous medium, α and D are the equivalent thermal and mass diffusivities of the porous medium, c_p is the specific heat of the fluid at constant pressure, q_r is the radiative heat flux, T and C are the temperature and concentration.

The boundary conditions at the surface are

$$y = 0 : \quad v = 0, \quad T_w = T_\infty + a x^n, \quad (5)$$

and at the infinity are

$$y \rightarrow \infty : \quad u = 0, \quad T \rightarrow T_\infty, \quad C \rightarrow C_\infty. \quad (6)$$

For heated surface, $a > 0$ and $b > 0$ in (5). Here T_∞ is a free stream temperature, C_∞ is the free stream concentration, T_w is surface temperature and C_w is the concentration at the surface.

Using the Rosseland approximation for radiation (Brewster [36]), one can write

$$q_r = -4 \frac{\gamma^*}{3k^*} \left(\frac{\partial T^4}{\partial y} \right), \quad (7)$$

where γ^* is the Stefan-Boltzmann constant and k^* is the mean absorption coefficient.

By using Rosseland approximation, the present analysis is limited to optically thick fluids. If the temperature differences within the flow are sufficiently small, then (7) can be linearized by expanding T^4 into the Taylor series about T_∞ , which after neglecting higher order terms takes the form

$$T^4 \approx 4 T_\infty^3 T - 3 T_\infty^4. \quad (8)$$

In view of (7) and (8), (3) reduces to

$$u \frac{\partial T}{\partial x} + v \frac{\partial T}{\partial y} = \left(\frac{k}{\rho c_p} + \frac{16\gamma^* T_\infty^3}{3\rho c_p k^*} \right) \frac{\partial^2 T}{\partial y^2}, \quad (9)$$

where k is fluid thermal conductivity and ρ is the density of the fluid.

To transform the equations (1)-(4) into a set of ordinary non-linear equations, the following transformations and dimensionless variables are introduced:

$$\eta = (R_a)^{\frac{1}{3}} \frac{y}{x}, \quad (10)$$

$$\psi = (R_a)^{\frac{1}{3}} \frac{k}{\rho c_p} f(\eta), \quad (11)$$

$$\theta(\eta) = \frac{T - T_\infty}{T_w - T_\infty}, \quad (12)$$

$$\phi(\eta) = \frac{c - c_\infty}{c_w - c_\infty}, \quad (13)$$

where $R_a = \frac{Kg\beta_T(T_w - T_\infty)x}{\alpha\nu}$ is the modified local Rayleigh number and ψ is the stream function such that

$$u = \frac{\partial \psi}{\partial y} \text{ and } v = -\frac{\partial \psi}{\partial x}.$$

In terms of the new variables, it is easy to show that the velocity components are given as

$$u = \alpha \left(\frac{Kg\beta_T a}{\alpha\nu} \right)^{\frac{2}{3}} x^{\frac{2n-1}{3}} f'(\eta), \quad (14)$$

$$\text{and } v = -\alpha \left(\frac{Kg\beta_T a}{\alpha\nu} \right)^{\frac{1}{3}} \left(\frac{n-2}{3} \eta f'(\eta) + \frac{n+1}{3} f(\eta) \right) x^{\frac{n-2}{3}}. \quad (15)$$

The equation (1) of continuity is identically satisfied by the above transformations, and (2)-(4) get reduced to the following nonlinear ordinary differential equations:

$$f'' + \left(n\theta + \frac{n-2}{3} \eta \theta' \right) + B \left(n\phi + \frac{n-2}{3} \eta \phi' \right) = 0, \quad (16)$$

$$\left(1 + \frac{4}{3} R_d \right) \theta'' - n f' \theta + \frac{n+1}{3} f \theta' = 0, \quad (17)$$

$$\phi'' - Le \left(n f' \phi - \frac{n+1}{3} f \phi' \right) = 0, \quad (18)$$

where $B = \frac{\beta_C(c_w - c_\infty)}{\beta_T(T_w - T_\infty)}$ (Buoyancy ratio), $Le = \frac{\alpha}{D}$ (Lewis number) and $R_d = \frac{4\gamma^* T_\infty^3}{3kk^*}$ (radiation parameter).

The parameter B measures the relative importance of mass and thermal diffusion in the buoyancy driven flow. It is clear that B is zero for thermal driven flow, positive for aiding flow and negative for opposing flow. It has been shown that the similarity solutions exist for the case of thermally driven flows (Cheng and Chang [1]).

On applying the similarity transformations, the boundary conditions (5) and (6) are changed to

$$\eta = 0: \quad f = 0, \quad \theta = 1, \quad \phi = 1, \quad (19)$$

$$\eta \rightarrow \infty: \quad f' = 0, \quad \theta = 0, \quad \phi = 0. \quad (20)$$

In the above equations and boundary conditions, the prime denotes differentiation with respect to the similarity variable η' .

III. INTEGRAL TREATMENT

The temperature and concentration profiles can be expressed in terms of the following exponential functions :

$$\theta(\eta) = \exp \left\{ -\left(\frac{\eta}{\delta_T}\right) \right\}, \quad (21)$$

$$\phi(\eta) = \exp \left\{ -\xi \left(\frac{\eta}{\delta_T}\right) \right\}, \quad (22)$$

which satisfy the boundary conditions (19) and (20).

Here δ_T is the arbitrary scale for the thermal boundary layer thickness, while ξ is its ratio to the concentration boundary layer thickness. The infinity is the boundary layer thickness for temperature as well as for concentration.

On integrating (16) with respect to η from $\eta = 0$ to $\eta = \infty$, and using the relations (21) and (22), we obtain the relation

$$f'(\eta) = \frac{2}{3}(n+1)\delta_T\theta - \left(\frac{n-2}{3}\right)\eta(\theta + B\phi) + \frac{2}{3}B(n+1)\frac{\delta_T}{\xi}\phi. \quad (23)$$

Thus, the non-dimensional velocity near the wall is given as

$$f'(0) = \frac{2}{3}(n+1)\delta_T + \frac{2}{3}B(n+1)\frac{\delta_T}{\xi}. \quad (24)$$

The transformed energy equation (17) and the constituent mass transfer equation (18) can be respectively integrated with respect to η from $\eta = 0$ to $\eta = \infty$, to obtain

$$\frac{1}{\delta_T^3} = \left(\frac{4n+1}{3}\right)\frac{1}{R_d^*} \left[\left(\frac{n+1}{3}\right) \left(1 + \frac{2B}{\xi(\xi+1)}\right) - \left(\frac{n-2}{3}\right) \left(\frac{1}{4} + \frac{B}{(\xi+1)^2}\right) \right], \quad (25)$$

and

$$\frac{1}{\delta_T^3} = \left(\frac{4n+1}{3}\right)\frac{Le}{\xi} \left[\left(\frac{n+1}{3}\right) \left(\frac{2}{\xi+1} + \frac{B}{\xi^2}\right) - \left(\frac{n-2}{3}\right) \left(\frac{1}{(\xi+1)^2} + \frac{B}{4\xi^2}\right) \right], \quad (26)$$

where $R_d^* = 1 + \frac{4}{3}R_d$.

The above equations govern the thermal boundary layer thickness for the coupled heat and mass transfer by natural convection from a horizontal surface embedded in a radiating Darcian fluid saturated porous medium.

The above two equations can be combined to obtain the algebraic equation

$$A_5\xi^5 + A_4\xi^4 + A_3\xi^3 + A_2\xi^2 + A_1\xi + A_0 = 0 \quad (27)$$

where $A_5 = 3n + 6$,

$A_4 = 6n + 12$,

$A_3 = 4(2B + 1)(n + 1) - (4B + 1)(n - 2) - 8LeR_d^*(n + 1)$,

$A_2 = 8B(n + 1) - 4LeR_d^*(B + 2)(n + 1) + LeR_d^*(B + 4)(n - 2)$,

$A_1 = -6B(n + 2)LeR_d^*$,

$A_0 = -3B(n + 2)LeR_d^*$.

As ξ is determined from (27), the local Nusselt and local Sherwood numbers, which are of main interest in terms of heat and mass transfer respectively, can be computed in the following manner:

The heat and mass transfer rates can be computed from

$$q = -k \left(\frac{\partial T}{\partial y}\right) \Big|_{y=0} \quad (28)$$

$$m = -D \left(\frac{\partial C}{\partial y}\right) \Big|_{y=0} \quad (29)$$

where q and m are local heat transfer and local mass transfer coefficients. With the help of (10)-(13), (28) and (29) can be rewritten as

$$q = k a^{\frac{4}{3}} \left(\frac{Kg\beta_T}{\alpha\nu}\right)^{\frac{1}{3}} \chi^{\frac{4n-2}{3}} (-\theta'(0)) \quad (30)$$

$$m = D b^{\frac{4}{3}} \left(\frac{\kappa g \beta T}{\alpha \nu} \right)^{\frac{1}{3}} x^{\frac{4n-2}{3}} (-\phi'(0)) \quad (31)$$

which show that q and m increase with x if $n > \frac{1}{2}$, decrease if $n < \frac{1}{2}$ and constant if $n = \frac{1}{2}$. The heat transfer coefficient in terms of the Nusselt number is given by

$$Nu = \frac{hx}{k} = \frac{qx}{k(T_w - T_\infty)} = -(Ra)^{\frac{1}{3}} \theta'(0)$$

where h is local heat flux.

$$\therefore \frac{Nu}{(Ra)^{\frac{1}{3}}} = \frac{1}{\delta_T} \quad [\text{from (21)}] \quad (32)$$

The mass transfer coefficient in terms of local Sherwood number is given by

$$Sh = \frac{mx}{D(C_w - C_\infty)} = -(Ra)^{\frac{1}{3}} \phi'(0)$$

$$\therefore \frac{Sh}{(Ra)^{\frac{1}{3}}} = \frac{\xi}{\delta_T} \quad [\text{from (22)}] \quad (33)$$

The thermal boundary layer thickness δ_T can be computed either from (25) or from (26).

IV. RESULTS AND DISCUSSION

To have a better insight into the physical problem, the results for velocity distribution, temperature and concentration near the horizontal surface have been presented in Fig.2 to Fig.10 and the dimensionless velocity, dimensionless temperature and concentration profiles have been shown in Fig.11 to Fig. 19 for various values of buoyancy ratio B , Lewis number Le and radiation parameter R_d^* . Before proceeding for a detailed study, our results have been validated by comparing them with the corresponding results of Cheng and Chang [1], Chang and Cheng [2] and Bansod et al. [16] by taking $Le = 1$, $B = 0$ and $R_d^* = 0$ (i.e. $R_d^* = 1$). The results have been found in good agreement as shown by table I. Also, our graphical results (Figs. 2 - 7) have been validated by comparing them with the corresponding results of Bansod et al. [16] by taking $R_d^* = 0$ (i.e. $R_d^* = 1$) and $0 \leq n \leq 2$. Bansod et al. [16] visited the problem by using shooting technique in conjunction with the Rung-Kutta fourth order method. The results have been found in excellent agreement.

In table II, numerical results have been presented for $f'(0)$, local Nusselt number and local Sherwood number for wide range of governing parameters B and Le and for selected values of power law exponent n keeping and $R_d^* = 1$. It is observed that for $B > 0$ (aiding flow) as Le increases, the heat transfer decreases. This is because a larger Le provides thicker thermal boundary layer. For $B < 0$ (opposing flow), an opposite trend is seen. When B is fixed, the mass transfer continuously increases along with increasing Le . It is further seen that velocity distribution increases in case of aiding flow while it shows a decreasing trend in case of opposing flow.

Figs. 2 and 3 show the variation of local Nusselt number and local Sherwood number with power law exponent n for fixed values of Le and R_d^* ($Le = 2$ and $R_d^* = 1$) and for different values of B . It is seen that both the local Nusselt and local Sherwood numbers increase with n . For aiding flow ($B > 0$), the local Nusselt number increases while the local Sherwood number decreases. Whereas, an opposite trend is observed in opposing flow ($B < 0$).

TABLE I. VALUES OF $Nu(Ra)^{-\frac{1}{3}}$ FOR $Le = 1, B = 0$ AND $R_d^* = 1$

n	Cheng and Chang [1]	Chang and Cheng [2]	Bansod et al. [16]	Present results
0.5	0.8164	0.8164	0.8164	0.8549
1.0	1.099	1.099	1.099	1.077
1.5	1.351	1.345	1.351	1.269
2.0	1.571	-	1.571	1.442

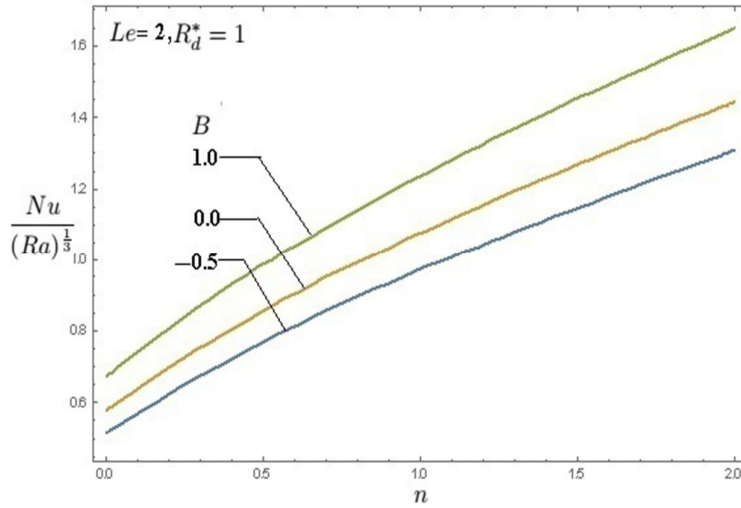


Figure 2. Variation of local Nusselt number for $R_d^* = 1$ and $Le = 2$

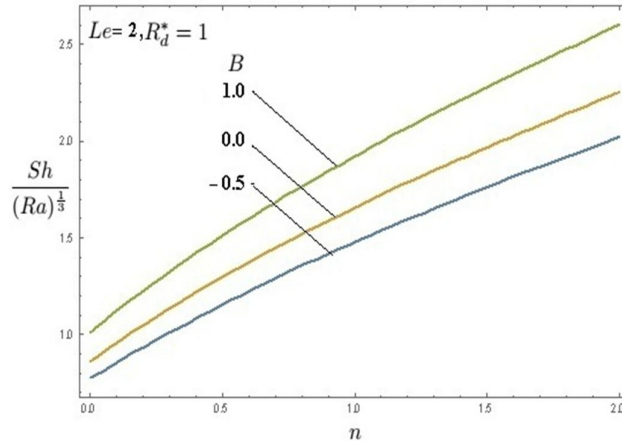


Figure 3. Variation of local Sherwood number for $R_d^* = 1$ and $Le = 2$

Figs. 4 and 5 give the variation of local Nusselt number and local Sherwood number with n for fixed values of B and R_d^* ($B = 1$ and $R_d^* = 1$) and for different values of Le . It is observed that the heat transfer decreases and mass transfer increases along with increasing Le .

Figs. 6 and 7 illustrate the effects of B and Le on velocity distribution near the horizontal surface with n by taking $R_d^* = 1$. It is found that the velocity distribution increases along with increasing and increasing B for fixed Le ($Le = 2$). But, for a fixed B ($B = 1$), the velocity distribution decreases along with increasing Le .

Figs. 8, 9 and 10 show the variation of local Nusselt number, local Sherwood number and $f'(0)$ with n for various values of R_d^* keeping Le and B fixed ($Le = 1, B = 1$). There occurs a decrease in heat transfer, an increase in mass transfer and an increase in velocity distribution with increasing radiation parameter R_d^* .

In Figs. 11 and 12, the dimensionless velocity profile $f'(\eta)$ shows changes of momentum boundary layer along with changes of B and Le . Figs. 13 and 14 show the corresponding response of the dimensionless temperature profile $\theta(\eta)$ and Figs. 15 and 16 show the corresponding response of the dimensionless concentration profile $\phi(\eta)$. It is seen that the thermal and concentration boundary layers shrink along with increasing B while along with increasing Le the concentration boundary layer shrinks more relative to the thermal boundary layer.

Figs. 17, 18 and 19 illustrate the changes of the dimensionless velocity profile, the dimensionless temperature profile and the dimensionless concentration profile for various values of R_d^* in aiding and opposing flows keeping $Le = 1$ fixed. It is found that, in case of aiding flow, the velocity distribution increases along with increasing R_d^* , whereas an opposing trend is observed for opposing flow. In both the cases of aiding and opposing flows, the temperature profile shows an increasing trend along with increasing R_d^* . Also, it is seen that the concentration boundary layer shrinks with increasing R_d^* for both aiding and opposing flows.

V. CONCLUDING REMARK

A detailed study has been carried out for heat and mass transfer by natural convection from a horizontal surface in a radiating Darcian fluid. The problem is solved by integral method of Von Karman type and numerical results have been verified with published results in case of heat transfer. It is seen that both heat and mass transfer rates increase with buoyancy ratio. More pronounced effect of the Lewis number is seen on the concentration field as compared to its effect on the flow and temperature fields. The mass transfer rate increases while the heat transfer rate decreases with increasing radiation parameter. The effect of radiation parameter on the flow field is more pronounced in aiding flow than in opposing flow. Whereas, the effect of radiation parameter is meagre on concentration field. Finally, the integral approach of Von Karman type adopted in this problem is very efficient and handy for making use of for engineering applications. Thus, the integral treatment remains a powerful means to attack boundary layer problems, since it naturally captures correct asymptotic behaviours as compared to the scale arguments which are not completely free from the risk of misinterpretation.

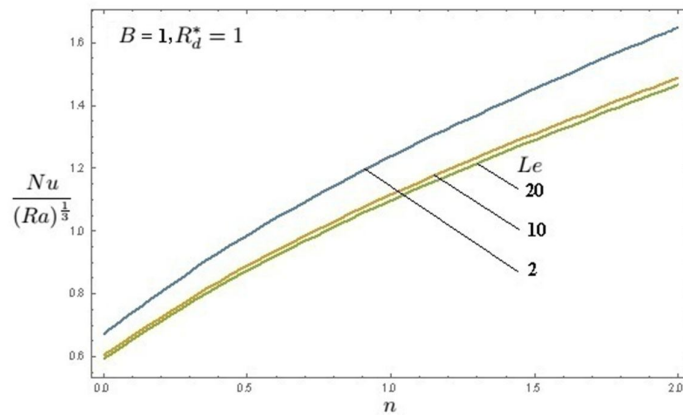


Figure 4. Variation of local Nusselt number for $R_d^* = 1$ and $B = 1$

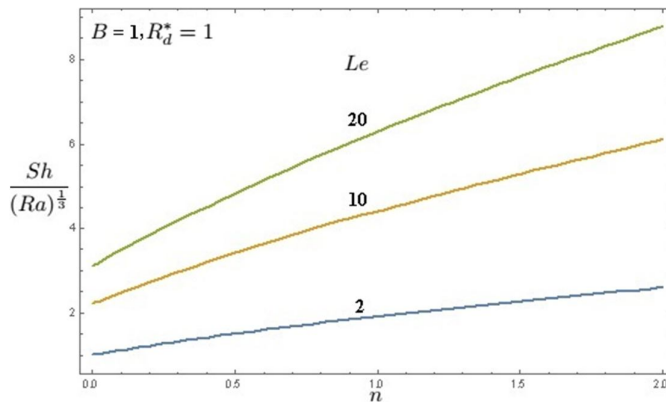


Figure 5. Variation of local Sherwood number for $R_d^* = 1$ and $B = 1$

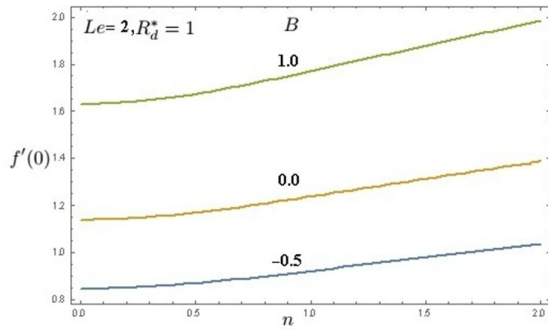


Figure 6. Variation of $f'(0)$ number for $R_d^* = 1$ and $B = 1$

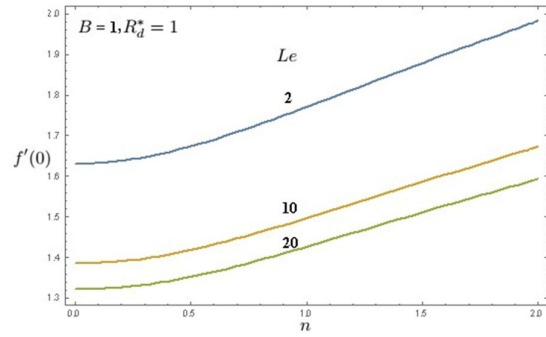


Figure 7. Variation of $f'(0)$ number for $R_d^* = 1$ and $B = 1$

TABLE II. SUMMARY OF INTEGRAL SOLUTION FOR $R_d^* = 1$

n	B	Le	$f'(0)$	$Nu(Ra)^{-\frac{1}{3}}$	$Sh(Ra)^{-\frac{1}{3}}$
0.5	4	1	3.4199	1.4620	1.4620
		5	2.3412	1.0499	2.8803
		10	2.0536	0.9636	3.9377
	0	1	1.1696	0.8549	0.8549
		5	1.1696	0.8549	2.1901
		10	1.1696	0.8549	3.1938
	-0.5	1	0.7368	0.6786	0.6786
		5	0.9789	0.8184	2.0575
		10	1.0329	0.8360	3.0634
1.0	4	1	1 3.619	1.8420	1.8420
		5	2.4722	1.3072	3.6725
		10	2.1642	1.2024	5.0537
	0	1	1.2378	1.0772	1.0772
		5	1.2378	1.0772	2.8254
		10	1.2378	1.0772	4.1499
	-0.5	1	0.7797	0.8549	0.8549
		5	1.0385	1.0347	2.6654
		10	1.0961	1.0557	3.9944
1.5	4	1	3.8415	2.1693	2.1693
		5	2.6197	1.5264	4.3635
		10	2.2901	1.4066	6.0317
	0	1	1.3137	1.2686	1.2686
		5	1.3137	1.2686	3.3841
		10	1.3137	1.2686	4.9940
	-0.5	1	0.8276	1.0069	1.0069
		5	1.1043	1.2214	3.2011
		10	1.1656	1.2451	4.8176
2.0	4	1	4.0548	2.4662	2.4662
		5	2.7616	1.7242	4.9947
		10	2.4117	1.5914	6.9270
	0	1	1.3867	1.4422	1.4422
		5	1.3867	1.4422	3.8963
		10	1.3867	1.4422	5.7690
	-0.5	1	0.8736	1.1447	1.1447
		5	1.1671	1.3909	3.6927
		10	1.2319	1.4170	5.5739

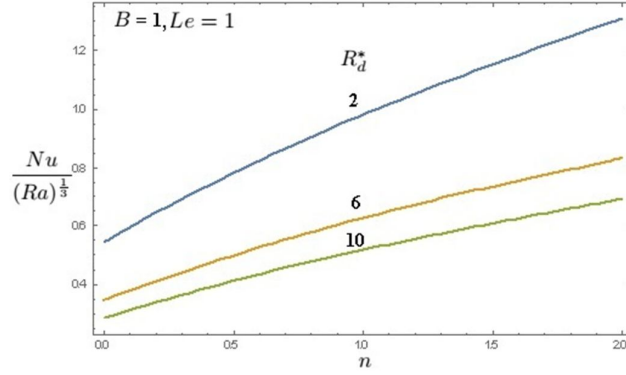


Figure 8. Variation of local Nusselt number for $Le = 1$ and $B = 1$

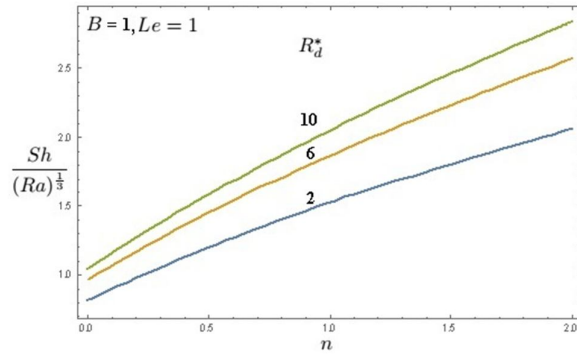


Figure 9. Variation of local Sherwood number for $Le = 1$ and $B = 1$

ACKNOWLEDGEMENT

One of the authors, namely, Ms. NasreenBano, is thankful to Dr. BabasahebAmbedkar Technological University, Lonere, for providing her the financial support in the preparation of the manuscript of the present paper under the aegis of World Bank funded Project TEQIP(Phase II).

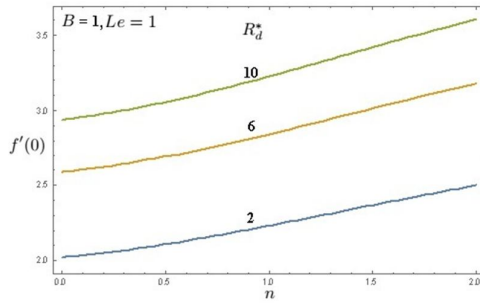


Figure 10. Variation of $f'(0)$ number for $Le = 1$ and $B = 1$

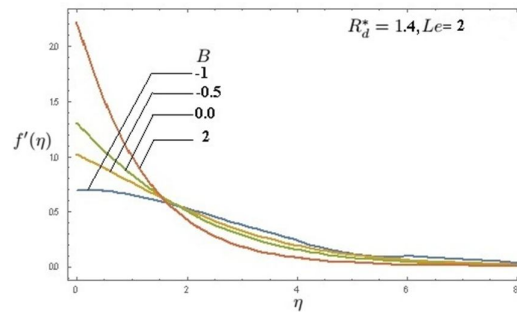


Figure 11. Dimensionless velocity profile for various values of B and $Le = 2$

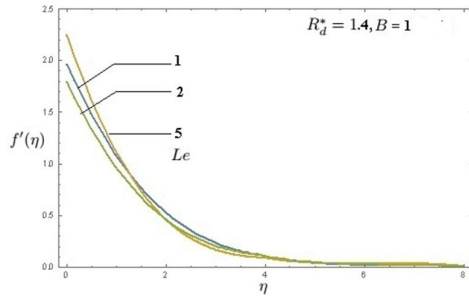


Figure 12. Dimensionless velocity profile for various values of Le and $B = 1$

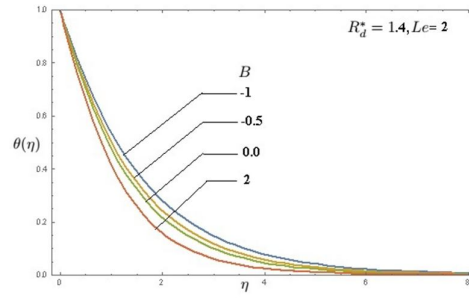


Figure 13. Dimensionless temperature profile for various values of B and $Le = 2$

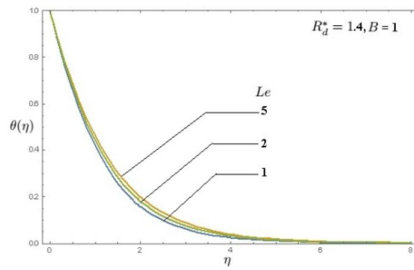


Figure 14. Dimensionless temperature profile for various values of Le and $B = 1$

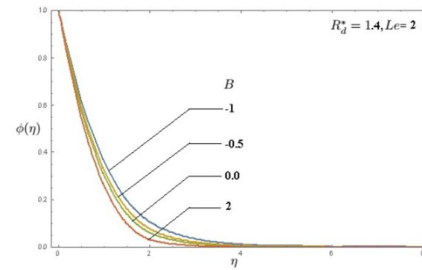


Figure 15. Dimensionless concentration profile for various values of B and $Le = 2$

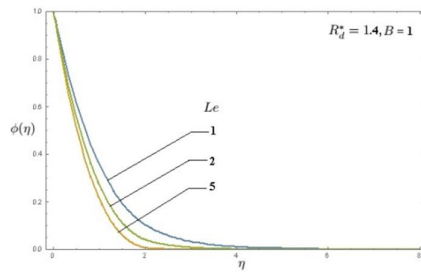


Figure 16. Dimensionless concentration profile for various values of Le and $B = 1$

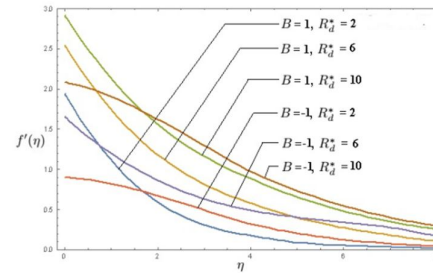


Figure 17. Dimensionless velocity profile for various values of R_d^* and $Le = 1$

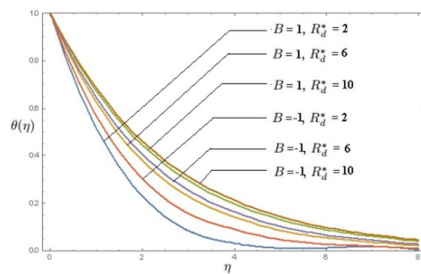


Figure 18. Dimensionless temperature profile for various values of R_d^* and $Le = 1$

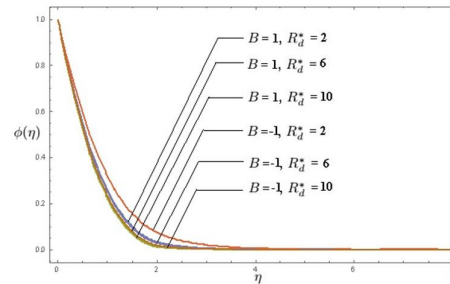


Figure 19. Dimensionless concentration profile for various values of R_d^* and $Le = 1$

REFERENCES

- [1] P. Cheng, and I. D. Chang, "Bouyancy induced flows in a saturated porous medium adjacent to the impermeable horizontal surfaces," *Int. J. Heat Mass Transfer*, vol. 38 pp. 1267-1272, 1976.

- [2] I. D. Chang, and P. Cheng, "Matched asymptotic expansion for free convection about an impermeable horizontal surface in a porous medium," *Int. J. Heat Mass Transfer*, vol. 26, pp. 163-174, 1983.
- [3] A. Bejan, and K. R. Khair, "Heat and mass transfer by natural convection in a porous medium," *Int. J. Heat Mass Transfer*, vol. 28 pp. 909-918, 1985.
- [4] J. Y. Jang, and W. J. Chang, "The flow and vertex instability of horizontal natural convection in a porous medium resulting from combined heat and mass buoyancy effects," *Int. J. Heat Mass Transfer*, vol. 31, pp. 769-777, 1988.
- [5] A. Yücel, "Heat and mass transfer about vertical surfaces in saturated porous media," *AIChE Symposium Series*, vol. 85, pp. 344-349, 1989.
- [6] A. Yücel, "Natural convection heat and mass transfer along a vertical cylinder in a porous medium," *Int. J. Heat Mass Transfer*, vol. 33, pp. 2265-2274, 1990.
- [7] O. V. Trevisan, and A. Bejan, "Combined heat and mass transfer by natural convection in a porous medium," *Adv. Heat Mass Transfer*, vol. 20, pp. 315-352, 1990.
- [8] A. Nakayama, and M. A. Hossain, "An integral treatment for combined heat and mass transfer by natural convection in a porous medium," *Int. J. Heat Mass Transfer*, vol. 38, pp. 761-765, 1995.
- [9] P. Singh, and O. Queeny, "Free convection heat and mass transfer along a vertical surface in a porous medium," *Acta Mech.*, vol. 123, pp. 69-73, 1997.
- [10] F. C. Lai, C. Y. Choi and F. A. Kulacki, "Coupled heat and mass transfer by natural convection from slender bodies of revolution in porous media," *Int. Commu. Heat Mass Transfer*, vol. 17, pp. 609-620, 1990.
- [11] F. C. Lai, and F. A. Kulacki, "Coupled heat and mass transfer from a sphere buried in an infinite porous medium," *Int. J. Heat Mass Transfer*, vol. 33, pp. 209-215, 1990.
- [12] F. C. Lai, "Coupled heat and mass transfer by natural convection from a horizontal line source in a saturated porous medium," *Int. Commu. Heat Mass Transfer*, vol. 17, pp. 489-499, 1990.
- [13] A. Nakayama, and T. Ashizawa, "A boundary layer analysis of combined heat and mass transfer by natural convection from a concentrated source in a saturated porous medium," *Appl. Sci. Res.*, vol. 56, pp. 1-11, 1996.
- [14] K. A. Yih, "Coupled heat and mass transfer by free convection over a truncated cone in porous media," *WVT/VVC or VHF/VMF ActaMechanica*, vol. 137, pp. 83-97, 1999.
- [15] A. J. Chamkha, and A. R. Khaled, "Non-similar hydromagnetic simultaneous heat and mass transfer by mixed convection from a vertical plate embedded in a uniform porous medium," *Numer. Heat Mass Transfer*, vol. 36, pp. 327-344, 1999.
- [16] V. J. Bansod, P. Singh, and B. V. Rathishkumar, "Heat and mass transfer by natural convection from a horizontal surface in a Darcian fluid," *Journal of Energy, Heat and Mass Transfer*, vol. 22, pp. 89-95, 2000.
- [17] A. J. Chamkha, and A. R. Khaled, "Hydromagnetic simultaneous heat and mass transfer by mixed convection from a vertical plate embedded in a stratified porous medium with thermal dispersion effect," *J. Heat Mass Transfer*, vol. 36, pp. 63-70, 2000.
- [18] P. Singh, O. Queeny and R. N. Sharma, "Influence of lateral mass flux on mixed convection heat and mass transfer over inclined surfaces in porous medium," *J. Heat Mass Transfer*, vol. 38, pp. 233-242, 2002.
- [19] V. J. Bansod, "The Darcy model of the boundary layer flows in a horizontal porous medium induced by combined buoyancy forces," *J. Porous Media*, vol. 6, pp. 273-281, 2003.
- [20] V. J. Bansod, "The effects of blowing and suction on double diffusion by mixed convection over inclined permeable surface," *J. Transport Porous Media*, vol. 60, pp. 301-317, 2005.
- [21] A. Postelnicu, "Influence of chemical reaction on heat and mass transfer by natural convection from vertical surfaces in porous media considering Soret and Dufour effects," *Int. J. Heat Mass Transfer*, vol. 43, pp. 595-602, 2007.
- [22] S. Shastri, "Thermal radiation and buoyancy effects on heat and mass transfer over a semi-infinite stretching surface with suction and blowing," *J. Appl. Math.*, Article ID 414830, 12 pages.
- [23] V. J. Bansod, and R. K. Jadhav, "An Integral treatment for combined heat and mass transfer by natural convection along a horizontal surface in a porous medium," *Int. J. Heat Mass Transfer*, vol. 52, pp. 2802-2806, 2009.
- [24] B. B. Singh, and I. M. Chandarki, "Integral treatment of coupled heat and mass transfer by natural convection from a cylinder in porous media," *Int. Commu. Heat Mass Transfer*, vol. 36, pp. 269-273, 2009.
- [25] O. A. Beg, T. A. Beg, A. Y. Bahier, and V. R. Prasad, "Chemically- reacting mixing convective heat and mass transfer along inclined and vertical plates with Soret and Dufour effects: Numerical solutions," *Int. J. Appl. Math. Mech.*, vol. 52, pp. 39-57, 2009.
- [26] V. J. Bansod, and R. K. Jadhav, "Effect of double stratification on mixed convective heat and mass transfer from a vertical surface in a fluid saturated porous medium," *J. Heat Transfer-Asian Research*, vol. 396, pp. 378-395, 2010.
- [27] S. S. Tak, R. Mathur, R. K. Gehlot, and A. Khan, "MHD free convection-radiation interaction along a vertical surface embedded in a Darcian porous medium in presence of Soret and Dufour effects," *J. Therm. Sci.*, vol. 14, pp. 137-145, 2010.
- [28] V. J. Bansod, and B. Ambedkar, "An integral treatment for combined heat and mass transfer by mixed convection along vertical surface in a saturated porous medium," *J. Mech. Engineering Res.*, vol. 35, pp. 138-151, 2011.
- [29] M. D. Clemente, A. Ianaro, G. Rufolo, and G. Cardone, "Hypersonic test analysis by means of aerothermal coupling methodology and IR thermography," *AIAA Journal*, vol. 51, pp. 1755-1769, 2013.

- [30] R. D. Cess, "The interaction of thermal radiation with free convection heat transfer," *Int. J. Heat Mass Transfer*, vol. 9, pp. 1269-1277, 1966.
- [31] A. Raptis, "Radiation and free convection flow through a porous medium," *Int. Comm. Heat Mass Transfer*, vol. 252, pp. 289-295, 1998.
- [32] M. A. Hossain, and H. S. Takhar, "Radiation effect on mixed convection along a vertical plate with uniform surface temperature," *Heat Mass Transfer*, vol. 31, pp. 243-248, 1996.
- [33] M. H. Mansour, "Radiative and free convection effects on the oscillatory flow past a vertical plate," *Astrophysics and Space Science*, vol. 166, pp. 26-35, 1990.
- [34] V. Ramachandra, Prasad, N. Bhaskar Reddy and R. Muthucumarswamy, "Radiation and mass transfer effects on two-dimensional flow past an impulsively started isothermal vertical plate," *Int. J. Thermal Science*, vol. 4612, pp. 1251-1258, 2007.
- [35] P. R. Babu, J. A. Rao, and S. Sheri, "Radiation effect on MHD heat and mass transfer flow over a shrinking sheet with mass suction," *J. Appl. Fluid Mechanics*, vol. 74, pp. 641-650, 2014.
- [36] M. Q. Brewster, *Thermal Radiative transfer and properties*, John Wiley and Sons, New York , 1992.